Sol-Gel Transition in Di-(2-ethylhexyl) phthalate-Plasticized Poly(vinyl chloride)

Chang Hyung Lee,[*] Jae-Woon Nah,[†] Kil-Won Cho,[‡] Seong Hun Kim,[§] and Airan Hahn[#]

Department of Medical Devices & Radiation Health, Korea Food & Drug Administration, 5 Nokbeon-dong, Eunpyung-gu, Seoul 122-704, Korea
[†]Department of Polymer Science and Engineering, Sunchon National University, Jeonam 540-742, Korea
[‡]Department of Chemical Engineering, Pohang University of Science and Technology, Pohang 790-784, Korea
[§]Department of Fiber & Polymer Engineering, Center for Advanced Functional Polymers, Hanyang University, Seoul 133-791, Korea
[#]Biotechnology & Environmenttal Eng. Div., Agency for Technology & Standards, #2 Joongang-dong, Kwancheon City, Gyeonggido 427-716, Korea
Received July 26, 2003

The gelation for di-(2-ethylhexyl) phthalate (DEHP)-plasticized poly(vinyl chloride) was studied by measuring time-resolved small-angle X-ray scattering (SAXS) and a flow of the solutions in test tube. It was found that for the gelation there were three regimes. At Regime I, the solution rapidly changed to a gel, and the SAXS intensity showed a peak and the peak intensity increased, keeping the peak angle constant. Applying the SAXS intensity to the kinetic analysis of the liquid-liquid phase separation, it was revealed that the spinodal decomposition proceeded to develop a periodic length of 29.9 nanometer in size, a hydrogen-bonding-type association in polymer rich phase followed, and then it induced fast gelation rate. At Regime II, the gelation slowly occurred and the SAXS intensity was not observed, suggesting that a homogeneous gel network was formed by a hydrogen-bonding. At regime III, the solution was a homogeneous sol.

Key Words : Sol-gel transition, DEHP-plasticized PVC, Small angle X-ray Scattering

Introduction

Di-(2-ethylhexyl) phthalate (DEHP)-plasticized poly(vinyl chloride) (PVC) is widely used in medical and pharmaceutical applications and have increased in use of medical devices such as tubings, blood containers, catheters and so on.[1-3] DEHP-plasticized PVC may be in contact with various kind of surrounding medium (SM) such as blood and manifold liquid medicine. When DEHP-plasticized PVC keeps in contact with a certain SM, DEHP may be leached from PVC articles into SM.[1,3,4] DEHP has been identified as one of the endocrine disruptors and there has been a controversy about its toxicity.[5] DEHP migration is due to the fact that DEHP does not react with PVC chemically, but permeate into PVC molecular chains physically, *i.e.*, PVC forms gel in DEHP. Therefore, gel structure could have a significant influence on DEHP migration. To control DEHP migration, we need to know the gelation process.

Until now a large number of reports have been published related to the DEHP-plasticized PVC gelation phenomenon,[6-9] and yet the glation mechanism is still not thoroughly elucidated. It is generally agreed that the gelation is the result of network formation. However, the nature of the tie points in the network is the subject of some controversy. It bas been suggested that gelation in DEHP-plasticized PVC is attributed to the tie formation of small crystallites.[7-9] This concept has been supported by extensive discussions on the gel melting behaviors in terms of the thermodynamics of the crystalline melting. Keller and co-workers have accumulated crystallographic evidence for the formation of crystallite in PVC gel.[10,11] However, gelation by crystallite formation is probably a phenomenon, which takes place at a very late stage of sol-gel transition. Furthermore, gel in DEHP-plasticized PVC is not visible with naked eye, indicating that gel morphology is in a range of nanometer. Therefore the purpose of the research described here is to investigate the gelation for the DEHP-plasticized PVC by time-resolved small angle X-ray scattering (SAXS) and a flow of the solutions in test tube.

Experimental Section

Materials. The PVC was obtained from Hanwha Chemical Co. and DEHP was purchased from Aldrich Co. The degree of polymerization of the PVC was 1,200, and DEHP was HPLC grade. The PVC and DEHP were mixed with various ratios. The samples that contain 30% or more PVC were prepared using Brabender twin-screw extruder and cut finely chopped. The rest of samples were mixed in beakers at 30-155 ^{o}C using magnetic stirrers.

Gel forming observation. Approximately 1g of the mixed sample were put into a test tube and were melted for 5 min at 170 ^{o}C to ensure homogeneity. The test tube was placed in an oil bath kept at a constant temperature. The sol-gel transition was observed at regular intervals by tilting the test tube. If a flow of the solutions in test tube is observed, this phenomenon is regarded a sol, and if not, gel. Visual

[*]To whom correspondence should be addressed. Phone: +82-2-380-1767; Fax: +82-2-380-1756; E-mail: c-hlee@kfda.go.kr

investigations on sol-gel transitions were carried out for solutions of various concentrations at temperatures ranging from 60 °C to 180 °C.

Time-resolved SAXS. The solutions was placed in a chamber set at a temperature and then transferred quickly into another chamber set at a desired isothermal temperature. Changes of the scattered intensity during the isothermal gelation were investigated by the time-resolved SAXS, employing synchrotron radiation; beam line 4C1 at Pohang Accelerator Laboratory, Pohang, Korea. The storage ring was operated at an Energy level of 2.5 GeV. The SAXS employs a point-focusiong optics with a Si Double crystal monochromator followed by a bent cylindrical mirror. The incident beam intensity of 0.149 nm wavelength *ë* was monitored by an ionization chamber for the correction of minor decrease of the primary beam intensity during the measurement.

Scattering intensity, *I*, was corrected for background scattering. Scattering intensity by thermal fluctuations was subtracted from the SAXS profile $I(q)$ by evaluating the slope of a $I(q)q^4$ *versus* q^4 plots[12] at wide scattering vectors q, where q is $(4\pi/\lambda)\sin\theta$, λ and 2θ, the wavelength and scattering angle, respectively. The data were corrected by the Lorentz equation (I^2 *vs.* q), with the intensity extrapolated to $q = 0$ and ∞. The correction for smearing effect by the finite cross section of the incident beam was not necessary for the optics of SAXS with point focusing

Results and Discussion

A sol-gel transition curve investigated by a flow of the solutions in test tube is shown in Figure 1. An open square and an open circle mean that the solution gelled after standing 10 min and 12 h, respectively. An open triangle means that the solution was still a sol. The sol-gel transition result so obtained divides into three regimes as labeled from I to III. The solution rapidly changes to a gel in Regime I, whereas the gelation in Regime II slowly occurs. In Regime III, the solution is a homogeneous sol. Gelation rate is found to be different in Regime I and Regime II. Then, we will confine discussion on gelation process to two gelation regions; *i.e.*, one is Regime I and another is Regime II.

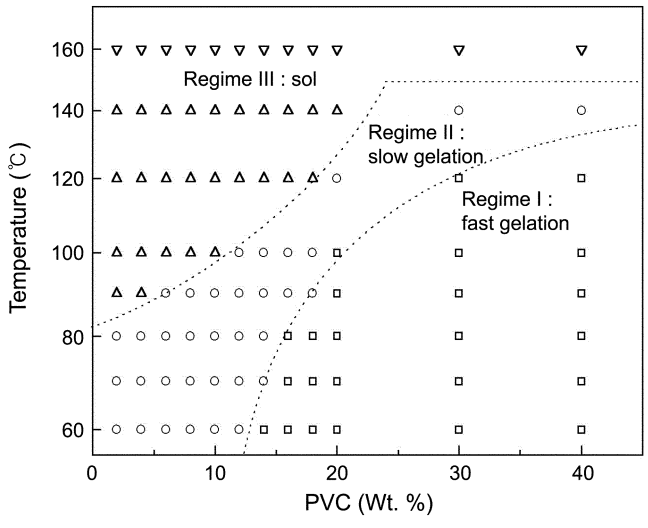

Figure 1. So-gel transition map of DEHP-plasticized PVC.

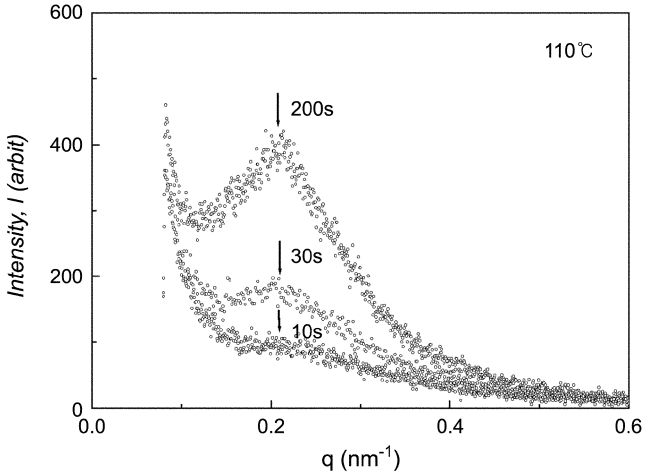

Figure 2. SAXS profiles of a 40/60 PVC/DEHP at gelated after 10, 30 and 100s.

To understand the origin of sol-gel transition, the time-resolved SAXS was carried out using synchrotron radiation. Figure 2 is a typical example of the change of the scattered intensity with time at various values of q during gelation in Regime I, where the magnitude of the scattering vector q is given by $q = (4\pi/\lambda)\sin(\theta/2)$. The scattering intensity I increases and shows a peak at $q = 0.21$ nm^{-1}, and the peak potion keeps constant. The periodic length (29.9 nm) is obtained by applying Bragg's law to the peak position of the SAXS profile. One may mention two possibilities about the origin of the peak: one is the long period between two adjacent crystalline lamellae and the other is the periodic length of the liquid-liquid (L-L) phase separation. The latter possibility seems to be more realistic, as the melting endotherm from crystalline lamellae in differential scanning calorimetry (DSC) heating trace was not observed. In DEHP-plasticized PVC, there is a report that DSC shows no exthorm from crystalline lamellar melting.[6] Then the scattering peak in SAXS is not attributed to the crystalline lamellae.

Supplemental evidence is clearly given by the shift of peak position during gellation. In general, the peak position, originated from crystalline lamellae, shifts to wide angle with crystallization, since the new lamellae is inserted interlamellar region with crytsallization. In Regime I, the peak position keeps constants (see Figure 2). Then it is concluded that the peak of the SAXS is assigned to the periodic length of the L-L density fluctuation.

The appearance of a scattering peak suggests that L-L phase separation occurs *via* spinodal decomposition mechanism. In order to better understand this point, we analyzed the early stage on the basis of the linearized theory.[13]

According to Cahn's linear theory of spinodal decomposition (SD), the scattering intensity I in the early stage of SD is expected to increase exponentially with time t;[13]

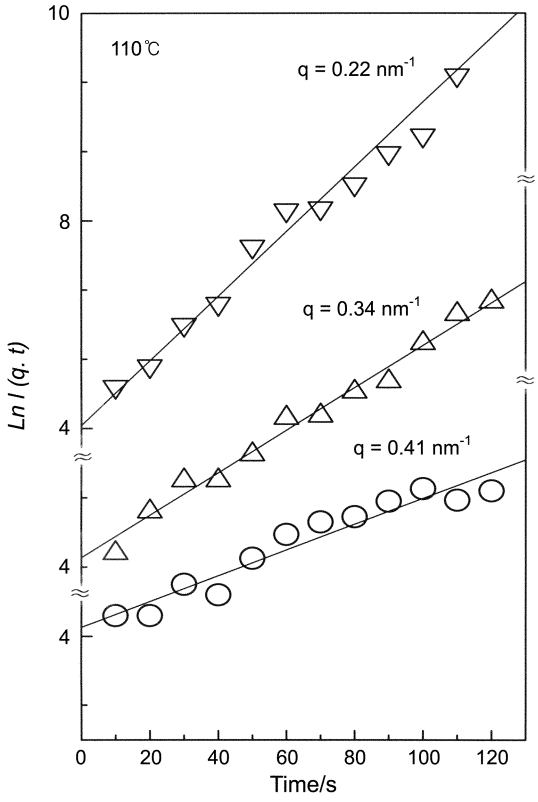

Figure 3. Change of the scattered intensity at various q with time for a 40/60 DEHP/PVC.

$$I(\boldsymbol{q}, t) = I(\boldsymbol{q}, 0)\exp[2R(\boldsymbol{q})t] \quad (1)$$

The amplification factor $R(\boldsymbol{q})$ is given by

$$R(\boldsymbol{q}) = -M\boldsymbol{q}^2(\partial^2 f/c^2 + 2\kappa\boldsymbol{q}^2) \quad (2)$$

where f is the local free energy of mixing, c is the concentration, κ is the concentration-gradient energy coefficient and M is the mobility. According to eq. 1, a plot of ln I *vs* time t at a fixed q should yield a straight line with slope of $2R(q)$. The linear relationship is realized for the L-L phase separation as shown in Figure 3, indicating that the initial stage can be described by the linearized theory.

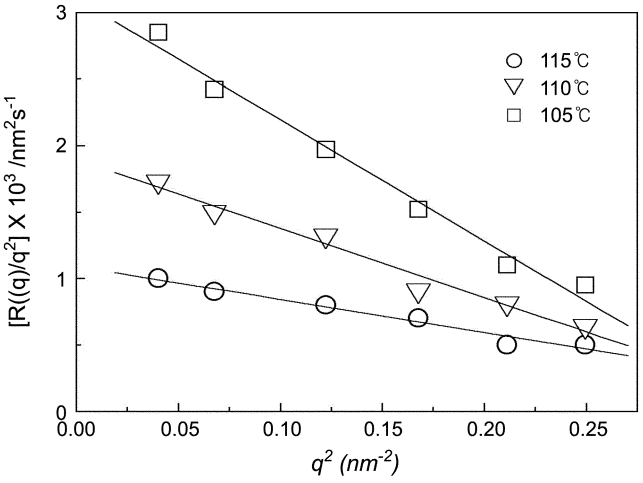

Figure 4. $R(q)q^2$ versus q^2 plot in a 40/60 PVC/DEHP.

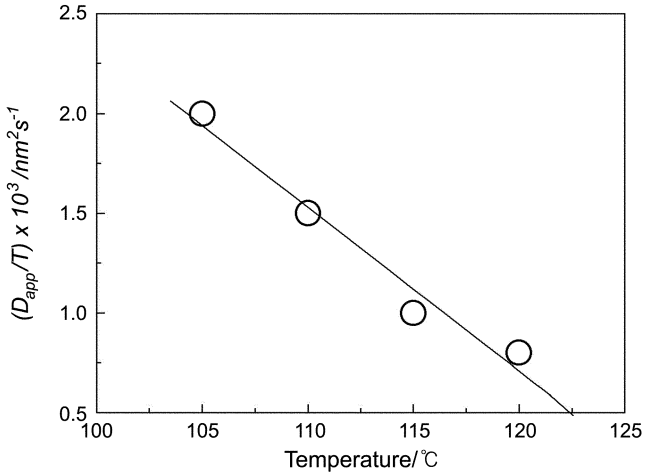

Figure 5. Temperature dependence of apparent diffusion coefficient D_{app} in a 40/60 PVC/DEHP.

Figure 4 shows $R(q)/q^2$ *vs* q^2. As expected from eq. 2, the plot yields a straight line, indicating again that this stage can be described with the framework of the linearized theory. From the interception of $R(q)/q^2$ at $q^2 = 0$, one can obtain apparent mutual diffusion coefficient D_{app} given by

$$D_{app} = -M(\partial^2 f/\partial c^2) \propto D_c[|\chi-\chi_s|/\chi_s] \propto T\,|\,T-T_s\,| \quad (3)$$

Where D_c is the self-diffusion coefficient for translational diffusion, χ is the interaction parameter, χ_s is the χ at the spinodal temperature and T_s is the spinodal temperature.

The values of D_{app} were obtained at various temperatures. The results are shown in Figure 5 as a function of temperature. D_{app} decreases with temperature. The dcreases in D_{app} with increasing temperature is expected in the UCST (upper critical solution temperature) system, since the quench depth $|\,T-T_s\,|$ decreases with temperature (see eq. 3). The increase in D_{app} was observed in the UCST system.[14] From these scattering studies, it is unambiguous that the phase diagram of the DEHP-plasticized PVC is of the UCST type as shown in dotted line in Figure 1. Therefore, we can speculate that, in Regime I, the gelation is accompanied by L-L phase separation through SD.

The peak position, indicative of periodic length caused by SD, was kept constant with time and its intensity increases (see Figure 2). It should be noted that no coarsening of the supermolecular structure was not observed in the late stages of L-L phase separation in Regime I, even after 12 h. These results suggest that further growth of L-L density fluctuation may be suppressed. This is explained by the immobilization of polymer chains that results from a hydrogen-bonding-type association in the polymer-rich phase *via* SD. Gelation inhibits coarsening. This type of behavior must be characteristic of the SD in solutions of gel-forming polymers.

Further evidence for gelation mechanism by SD is given by reverse temperature-jump experiment. The gelated specimen at 110 °C for 240s was subject to a temperature-jump to 150 °C for the gel dissolution. Figure 6 shows typical decays of the scattered intensities with various q during gel dissolu-

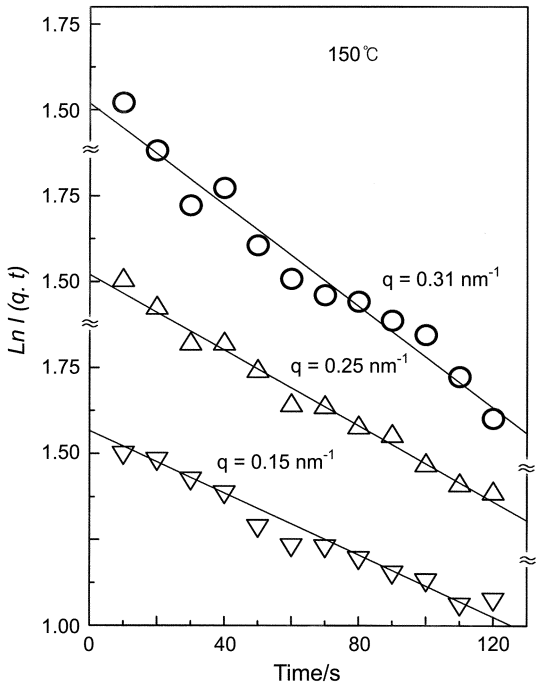

Figure 6. Change of the scattered intensity at various q with time for a 40/60 DEHP/PVC during gel dissolution at 150 °C.

tions for a reverse jump experiment. The decay rate of the scattered intensity $2R(q)$ was determined from the slopes in Figure 6. The data indicate that $R(q)/q^2$ is proportional to q^2 (see Figure 7). This decay phenomenon typically appeared in L-L phase separation system formed by SD.[15]

On the basis of the above results, the following conclusions can be drawn. At regime I, the SD proceeds to develop a periodic length of 29.9 nanometer in size, a hydrogen-bonding type association in polymer rich phase follows, and then it induces fast gelation rate. As has been already mentioned, SD results in the development of the interconnected structure of polymer-rich and polymer-poor regions. In our PVC system, it is fairly fast rate process and gelation follows. Therefore, when gelation takes place in a polymer-rich region, the whole system should be gelled unless the connectivity of the polymer-rich region is interrupted. The fast gelation prevents further spinodal decomposition. The rate of gelation increases with PVC composition so that the PVC rich phase in L-L phase separation is gelated. The gelation prevents the mobility and then L-L spinodal decomposition retards. Finally the spinodal decompositions stops.

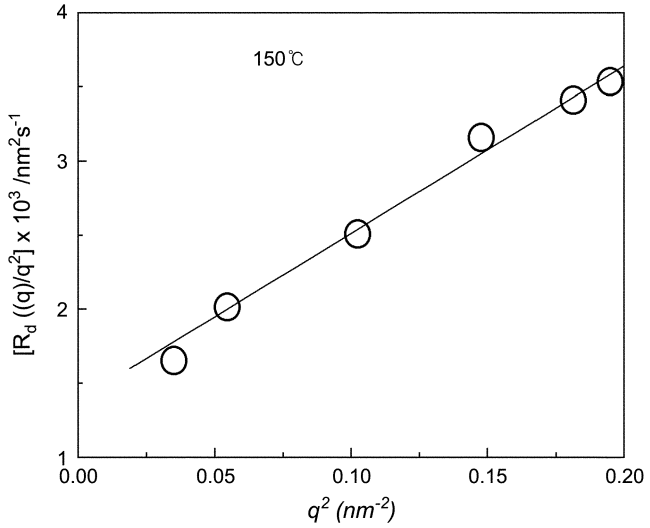

Figure 7. q^2 dependence of decay rate $R(q)$ of a 40/60 PVC/DEHP.

In regime II, the SAXS intensity was not observed during gelation. This means that density fluctuation in a range of nanometer is not developed. Gelation takes place without L-L phase separation, *i.e.*, the mechanism of the gelation is different from that in Regime I. This mechanism is probably due to a hydrogen-bonding type association. Hydrogen bonding has been referred to as the reason for the formation of the physical network.[16] Their results showed that hydrogen bonding between Cl and H is responsible for the gel state. From the above results, it is interpreted that, in regime II, gelation by hydrogen bonding first proceeds, and then mobility of the molecule is retarded so that no density fluctuation such as L-L separation takes place. This mechanism must result in a homogeneous gel network

Conclusions

By a series of time-resolved SAXS and a flow of the solutions in test tube, it was revealed that the phase diagram in DEHP-plasticized PVC was of UCST and consistent with sol-gel transition curve, and the sol-gel transition curve was divided into three distinct regimes as labeled from I to III. In Regime III, the solution was a homogeneous sol, whereas it was gelated in Regime I and II. In Regime II, the gelation was attributed to a hydrogen-bonding, which resulted in a homogeneous gel network. In Regime I, the gelation was accompanied by L-L phase separation through spinodal decomposition and it was supported by time-resolved SAXS analysis.

Acknowledgment. Synchrotron SAXS experiments were performed at the Pohang Light Source (4C1 beam line) in Korea, which was supported by MOST and Pohang Iron and Steel Co. (POSCO).

References

1. Jayakrishnan, A.; Sunny, M. C. *Polymer* **1996**, *37*, 5213.
2. Kambia, K.; Dine, T.; Azar, R.; Gressier, B.; Luyckx, M.; Brunet, C. *Int. J. Pharm.* **2001**, *229*, 139.
3. Jacobson, M. S.; Kevy, S. V.; Parkman, R.; Wesolowski, J. S. *Transfusion* **1980**, *20*, 443.
4. Papaspyrides, C. D.; Duvis, T. *Polymer* **1990**, *31*, 1085.
5. Kambia, K.; Dine, T.; Azar, R.; Gressier, B.; Luyckx, M.; Brunet, C. *Int. J. Pharm.* **2001**, *229*, 139.
6. Soenen, H.; Nerghmans, H. *J. Polym. Sci.; Part B; Polym. Phys.* **1996**, *34*, 241.
7. Jujin, J. A.; Gisolf, J. H.; de Jong, W. A. *Kollid Z. Z. Polym.* **1973**, *251*, 456.
8. Najeh, M.; Munch, J. P.; Guenet. *Macromolecules* **1992**, *25*, 7078.

9. Yang, Y. C.; Geil, P. H. *J. Macromole. Sci., Phys.* **1987**, *B22*, 980.
10. Guerrero, S. J.; Keller, A. *J. Macromole. Sci., Phys.* **1981**, *B20*, 161.
11. Guerrero, S. J.; Keller, A. *J. Macromole. Sci., Phys.* **1981**, *B20*, 167.
12. Koberstein, J. K.; Morra, B.; Stein, R. S. *J. Appl. Crystallogr.* **1980**, *13*, 34.
13. Chan, J. W. *J. Chm. Phys.* **1965**, *42*, 93.
14. Hashimoto, T.; Kumaki, J.; Kawai, H. *Macromolecules* **1983**, *16*, 641.
15. Lee, H. S.; Kyu, T. *Macromolecules* **1990**, *23*, 459.
16. Yang, Y. C.; Geil, P. H. *J. Macromole. Sci., Phys.* **1983**, *B20*, 463.